Ecotoxicology and Environmental Safety 129 (2016) 199–209

Contents lists available at ScienceDirect

Ecotoxicology and Environmental Safety

journal homepage: www.elsevier.com/locate/ecoenv

An exploration of spatial human health risk assessment of soil toxic metals under different land uses using sequential indicator simulation

Jin-hui Huang [a,b,*], Wen-chu Liu [a,b], Guang-ming Zeng [a,b,*], Fei Li [a,c], Xiao-long Huang [a,b], Yan-ling Gu [a,b], Li-xiu Shi [a,b], Ya-hui Shi [a,b], Jia Wan [a,b]

[a] College of Environmental Science and Engineering, Hunan University, Changsha 410082, China
[b] Key Laboratory of Environmental Biology and Pollution Control (Hunan University), Ministry of Education, Changsha 410082, China
[c] School of Information and Safety Engineering, Zhongnan University of Economics and Law, Wuhan 430073, China

ARTICLE INFO

Article history:
Received 27 November 2015
Received in revised form
21 March 2016
Accepted 23 March 2016
Available online 2 April 2016

Keywords:
Soil
Toxic metals
Land use
Sequential indicator simulation
Health risk assessment

ABSTRACT

A modified method was proposed which integrates the spatial patterns of toxic metals simulated by sequential indicator simulation, different exposure models and local current land uses extracted by remote-sensing software into a dose-response model for human health risk assessment of toxic metals. A total of 156 soil samples with a various land uses containing farm land (F1–F25), forest land (W1–W12) and residential land (U1–U15) were collected in a grid pattern throughout Xiandao District (XDD), Hunan Province, China. The total Cr and Pb in topsoil were analyzed. Compared with Hunan soil background values, the elevated concentrations of Cr were mainly located in the east of XDD, and the elevated concentrations of Pb were scattered in the areas around F1, F6, F8, F13, F14, U5, U14, W2 and W11. For non-carcinogenic effects, the hazard index (*HI*) of Cr and Pb overall the XDD did not exceed the accepted level to adults. While to children, Cr and Pb exhibited *HI* higher than the accepted level around some areas. The assessment results indicated Cr and Pb should be regarded as the priority pollutants of concern in XDD. The first priority areas of concern were identified in region A with a high probability (>0.95) of risk in excess of the accepted level for Cr and Pb. The areas with probability of risk between 0.85 and 0.95 in region A were identified to be the secondary priority areas for Cr and Pb. The modified method was proved useful due to its improvement on previous studies and calculating a more realistic human health risk, thus reducing the probability of excessive environmental management.

© 2016 Elsevier Inc. All rights reserved.

1. Introduction

At present, over half of the global population lives in urbanized areas (United Nations, 2014). Toxic metals contamination in soils has become a serious environmental problem around the world because of their potential impact to soil properties, soil biological activity and effective supply of nutrients, especially in the developing countries associated with their rapid progress of industrialization and urbanization (Guney et al., 2010; Qu et al., 2013a). In addition, soil toxic metals can be strongly enriched through the food chain or other ways, which threatens human health via direct inhalation, ingestion and dermal contact absorption (Boularbah et al., 2006; Komnitsas and Modis, 2009; Li et al., 2013; Saleem et al., 2014; Yuan et al., 2014). Therefore, to scientifically and effectively assess the potential risk of soil toxic metals to human health is of great importance to environmental management decision making.

In recent years, increasing studies have quantitatively evaluated the health risks of human exposure to soil toxic metals with single evaluation models (Lim et al., 2009; Wang et al., 2014; Cai et al., 2015; Li et al., 2015c). To preserve the spatial distribution of the risk, some studies used the geostatistical interpolation, like inverse distance weighted, kriging, or indicator kriging to evaluate the toxic metals concentrations in soils in the process of human health risk assessment (Guo et al., 2012; Li et al., 2014; Zhao et al., 2014; Xiao et al., 2015). And by comparing the calculation results with a regulatory cutoff level deemed 'safe' or 'acceptable', some studies have identified the priority pollutants/regions and provided initial risk management measures (Korre et al., 2002; Simasuwannarong and Satapanajaru, 2012; Ji et al., 2013). However, according to some researches in recent years, there are some deficiencies in the assessment process. Firstly, the smoothing effect, which results in less variation in estimated values than in

* Corresponding authors at: College of Environmental Science and Engineering, Hunan University, Changsha 410082, China.
E-mail addresses: huangjinhui_59@163.com (J.-h. Huang), zgming@hnu.edu.cn (G.-m. Zeng).

http://dx.doi.org/10.1016/j.ecoenv.2016.03.029
0147-6513/© 2016 Elsevier Inc. All rights reserved.

observed values, was commonly found in the maps produced by optimal interpolation (Juang et al., 2004; Zhao et al., 2005; Modis et al., 2008; Zeng et al., 2009; Qu et al., 2013b). This problem causes large value to be underestimated and small values to be overestimated, and such effect can be transferred into the subsequent health risk assessment modeling, thereby considerably impacting on the results of the health risk assessment (Zhao et al., 2008; Qu et al., 2013a). Secondly, few studies took land use types into account in the process of health risk assessment. The pathways and receptors are different for each land use, so the land use types are in close relationship with the human health risk (Xu et al., 2008; Cheng and Nathanail, 2009; Zhao et al., 2012; Islam et al., 2015). The neglect of land use types may result in an overestimation of human health risk and consequently lead to an excessive environmental management. Finally, the risk management measures proposed in the previous studies were often inflexible and not practical. These inflexible risk management measures could neither satisfy the requirements of efficient environmental risk management in consideration of cost-benefit, nor meet the social economic demands of most developing countries like China.

To address some of these problems, a modified method is proposed which takes the spatial distribution and local uncertainty of concentrations of toxic metals into account by using SIS and incorporates different exposure models and current land use types extracted by remote-sensing software together to assess

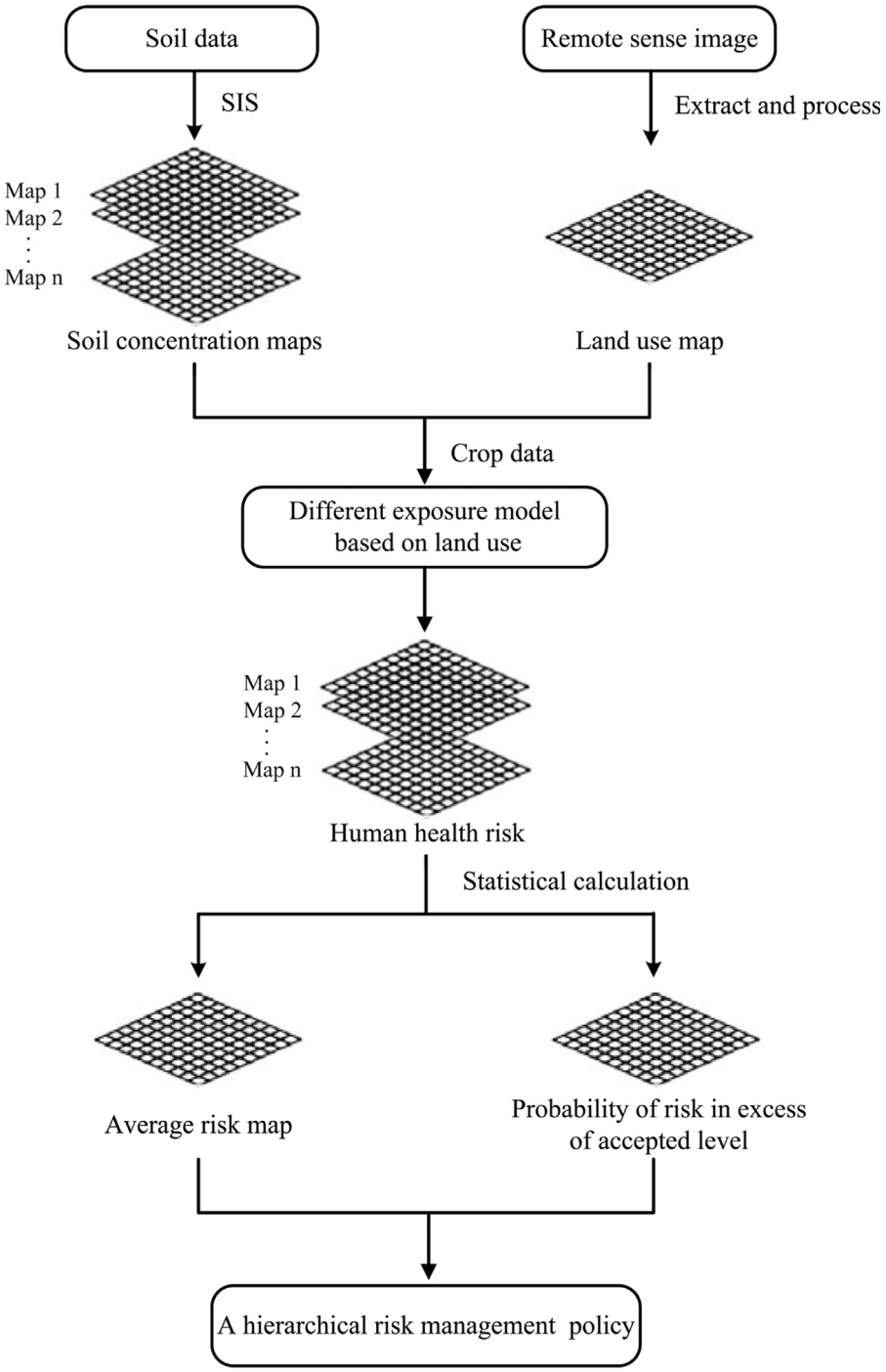

Fig. 1. Flow chart of the steps for the modified human health risk assessment of soil toxic metals under different land uses using SIS.

the risk of human exposure to toxic metals. At the same time, a hierarchical risk management policy is proposed to provide reference for flexible and cost-efficient risk management policy-making. The objective of this study is: (1) to investigate and simulate spatial distributions of toxic metals (Cr and Pb) in topsoil from the study area; (2) to explore the spatial potential risk of toxic metals (Cr and Pb) in soil to human health associated with different land uses; (3) to accuracy identify the priority pollutants/regions of concern using non-carcinogenic health risk assessment models associated with the probability of risk in excess of the accepted level.

2. Materials and methods

2.1. Procedure for the human health risk assessment

The aim of this study is to explore a modified spatially-evaluated method for assessing risks of human exposure to toxic metals in soil. There are three main aspects together that make this method novel. First, sequential indicator simulation (SIS) (Deutsch and Journel, 1998) are used to preserve the spatial distribution and local uncertainty in the estimates (Gay and Korre, 2006, 2009). Second, risks incorporating different exposure models and current land use types in the study area are calculated, providing a more realistic assessment. Finally, results can be mapped to show the area with risks exceeding the accepted level and its corresponding probability of risk, and a hierarchical risk management policy can be proposed to provide reference for flexible and cost-efficient risk management policy-making. The procedure for the human health risk assessment method involves the following steps (Fig. 1): (1) simulate a series concentrations of toxic metals in topsoil based on the original data using the GSLIB90 SISIM routine (Deutsch and Journel, 1998) on a designed square grid; (2) extract the present land use map in the study area using the remote-sensing software and then divide the image into the designed grids using the ArcGIS 9.3 to link to the simulation results of toxic metals; (3) calculate a series risk of human exposure to toxic metals based on the simulation concentrations of toxic metals in topsoil and its corresponding rasterized land use; (4) map the E-type risk map (average risk) of toxic metals to human health to have a knowledge of the risks distribution trend of toxic metals and identify priority pollutants and hazardous zone preliminary; (5) for the priority pollutants, map the probability of risk in excess of the accepted level to assess the reliability of delineating the hazardous zone based on the uncertainty of each single location; (6) provide a hierarchical risk management policy based on the E-type risk map and its probability of risk map.

2.2. Study area

Xiandao District (XDD), a municipal district of Changsha city, is located on the West Bank of Xiangjiang, covering a total area of approximately 1200 km^2 and having a total population of over 1.2 million. The major types of industry in XDD are mining, machinery, metallurgy, chemical and production of building materials (Chen et al., 2011; Li et al., 2015a; Huang et al., 2016). In 2007, XDD is approved by the Chinese State Council as the pilot district to explore how to construct resource conservation and environment friendly society in a China. Therefore, XDD was selected as the study area (Fig. 2) which has been experiencing rapid urbanization and economic development with an obvious decline of environmental quality in recent years (Li et al., 2015a; Huang et al., 2016).

2.3. Sampling and chemical analysis

A total 156 samples (3 parallel samples for each sampling site) were collected from the upper soil layer (0–20 cm) at 52 sample sites with a various land uses containing farm land (F1–F25), forest land (W1–W12) and residential land (U1–U15) in October 2013. Soil samples sites were set to correspond to a 5×5 km grid. At each sampling point, five sub-samples from nearby 5 m^2 area (MAPRC, 2006; Xi et al. 2004) were randomly taken using a stainless steel auger and then mixed to a composite soil sample. About 0.5 kg soil samples were collected in plastic bags and brought back to the laboratory for analysis. In the laboratory, soil samples were air-dried at room temperature and ground with an agate grinder to pass a 0.15 mm nylon sieve (MAPRC, 2006; Xi et al., 2004). All the soil samples were stored in brown bottles at room temperature prior to laboratory analysis. Soil pH, Soil organic matter, Cation exchange capacity (CEC) and Soil mechanical composition were analyzed (Li et al., 2015b). All the soil samples were digested with HNO_3, HF, and $HClO_4$, and the total Cr and Pb in soils were analyzed by an atomic absorption spectrophotometer

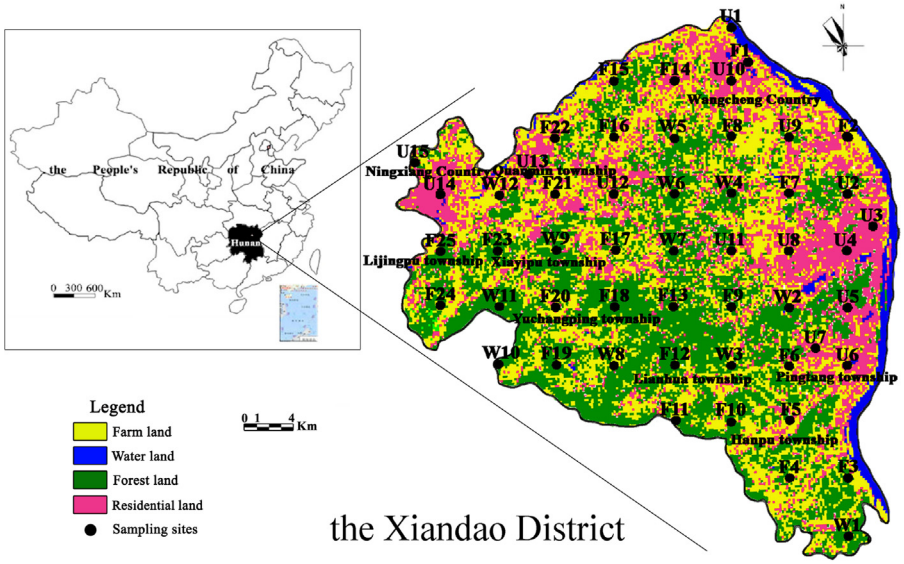

Fig. 2. Sampling sites in Xiandao District. The left image is map of China; the right image is a rasterized (200 × 200 m) map of XDD in which different land use types are labeled.

(AAnalyst-700, Perkin-Elmer Inc., US).

For the quality control, reagent blanks and State first-level standard materials (GBW GSS-5) for soils were set in each batch of samples to verify the accuracy and precision of the digestion procedure and subsequent analysis. The analysis results were reliable when repeat sample analysis error was below 5%, and the analytical precision for replicate samples was within ± 10%. The results met the accuracy demand of the Chinese Technical Specification for Soil Environmental Monitoring HJ/T 166-2004.

2.4. Human health risk assessment based on land use

The health risk assessment models [(Eqs. (1)–(4)] used in present study to evaluate the exposure risk of toxic metals to children (up to 12 years old) and adults under different land uses are based on models referring to the US Environmental Protection Agency (US EPA, 1989, 1996). In this study, soil and food were used as the sources to calculate the exposure doses of toxic metals. Human beings may be exposed to toxic metals mainly via the following four pathways: (1) direct ingestion of soil particles, (2) dermal contact absorption, (3) inhalation of suspended soil particles though mouth and nose, (4) diet through the food intake. The daily exposure dose of toxic metals via various exposure pathways can be calculated as follows:

$$Dose_{oral-soil} = \frac{C_{soil} \times IR_{ing} \times ED \times EF}{BW \times AT} \times 10^{-6} \quad (1)$$

$$Dose_{der-soil} = \frac{C_{soil} \times SA \times SL \times ABS \times ED \times EF}{BW \times AT} \times 10^{-6} \quad (2)$$

$$Dose_{inh-soil} = \frac{C_{soil} \times IR_{inh} \times ED \times EF}{PEF \times BW \times AT} \quad (3)$$

$$Dose_{oral-food} = \frac{C_{veg} \times IR_{veg} \times ED \times EF}{BW \times AT} + \frac{C_{rice} \times IR_{rice} \times ED \times EF}{BW \times AT} \quad (4)$$

where $Dose_k$ is the daily exposure dose of toxic metals via k exposure pathways, mg/(kg · d); C_{soil} is the simulated concentration of toxic metal in topsoil from XDD, mg/kg; C_{veg} and C_{rice} are the concentrations of toxic metal in vegetable and rice, respectively, mg/kg, fresh weight. All the parameters associated with risk assessment were showed Table S1, and in order to decrease the parameter uncertainty and ensure the accuracy of the assessment, the local parameters including *BW*, *SA*, *EF*, *ED*, *SL*, IR_{veg}, IR_{rice} and *AT* were adopted.

The hazard quotient (*HQ*) is used to assess the non-cancer risk from toxic metals, which was determined by the ratio of the daily exposure dose of toxic metals to its relative reference dose (*RfD*). The hazard index (*HI*) is presented as the sum of more than one *HQ* for multiple exposure pathways of each toxic metal. The human health risk can be assessed by the *HI*. If the *HI* value is greater than 1, there is a chance that non-carcinogenic may occur; if the *HI* value is less than 1, the reverse applies. The degree of risk increases as *HI* increases (US EPA, 2002; MEPPRC, 2014). The *HQ* and *HI* of toxic metals can be calculated as follows:

$$HQ_i = \frac{Dose_i}{RfD_i} \quad (5)$$

$$HI = \sum_{i=1}^{n} HQ_i \quad (6)$$

where RfD_i is the corresponding reference dose of different exposure pathways for each toxic metal, mg/(kg · d). The oral reference dose (RfD_{oral}) for Cr and Pb were 3.00E-03 and 3.50E-03 mg/(kg · d), respectively; The dermal reference dose (RfD_{der}) for Cr and Pb were 6.00E-05 and 5.25E-04 mg/(kg · d), respectively; The inhalation reference dose (RfD_{inh}) for Cr and Pb were 2.86E-05 and 3.52E-04 mg/(kg · d), respectively. All the reference dose (RfD_i) values of the studied metals were adopted to the Integrated Risk Information System (US Department of Energy, 2004).

As the exposure pathways and receptors are different for each land use, the land use is taken into account during the health risk assessment. Present land use mapping in the study area was determined from a remote sensing image of XDD. Landsat 7 image, acquired on January in 2014, with pixel resolution at 30 m, was as the source for this work (Li et al., 2015b). The original images were extracted using the remote-sensing software ENVI 4.7 (ITT Visual Information Solutions Inc.). Associated with the land use map in 2011 and the land use planning map in 2013 of XDD established by the Hunan government, the study area was divided into four land uses including farm land (34.6%), forest land (31.7%), residential land (32.6%) and water area (1.1%) based on their remote-sensing spectral characteristics. On the local farm and residential land, toxic metals can enter the human body via direct ingestion of soil particles, dermal contact absorption, diet through the food intake and inhalation of suspended soil particles. On the local forest land, toxic metals can enter the human body via ingestion of soil particles, dermal contact absorption and inhalation of soil particles. For the reason that the water areas accounts for a small area of XDD, the human health risk associated with the water area was not taken into account in this study. In consideration of the area of XDD, the accuracy of health risk assessment, the time-cost and hardware requirement of the simulation (Figs. S1 and S2), the image layer was divided into 200 × 200 m grids in this study using the ArcGIS 9.3 to link to the simulated metal concentrations in soils. Furthermore, considering that multiple land uses may exist in a gird, the land use in each grid was determined by the predominant land use in that grid (Fig. 2).

2.5. Exposure media concentrations

Considering that rice cultivation is the main agricultural activities in XDD, we took the heavy metals in rice and vegetable as the sources of human health risk via food intake pathway (Guo et al., 2010). The toxic metal concentrations in crops referred to the relevant literature and considered to be 0.18 and 0.064 mg/kg for Cr, and 0.21 and 0.14 mg/kg for Pb in rice and vegetable, respectively (Liu and Chen, 2004; Li et al., 2005; Liu et al., 2005; Lei et al., 2010). The toxic metal concentration data in soils were treated spatially and probabilistically using the SIS, for its spatial variability and local uncertainty. SIS is a most widely used indicator-based stochastic simulation method, with no assumption required about the distribution model of observed data (Goovaerts, 1997; Juang et al., 2004). At the same time, this method takes into account not only the spatial variation of observed data at sampled locations but also the variation in estimations at unsampled locations. Instead of producing a map of best local estimates, the SIS produces a series feasible maps and each one matches the sample statistics, variogram model and conditioning (sample) data reasonably. The SIS algorithm is employed as follows (Goovaerts, 1996, 1997; Deutsch and Journel, 1998; Juang et al., 2004):

(1) Transform the data of soil toxic metals concentrations into the indicator codes by the indicator function $I(x; z_k)$, which is under a desired cutoff value z_k:

$$I(x; z_k) = \begin{cases} 1, & if\ z(x) \le z_k \\ 0, & otherwise \end{cases} \quad (7)$$

(2) Obtain several indicator variograms respectively corresponding to the given cutoff values z_k according to Eq. (8):

$$\gamma_I(h) = \frac{1}{2N(h)} \sum_{i=1}^{N(h)} \left[I(x_i; z_k) - I(x_i + h; z_k) \right]^2 \quad (8)$$

where h is the distance between locations x_i and x_i+h, and $N(h)$ is the number of data pairs for x_i and x_i+h.

(3) Divide the whole studied region into the grids at a defined size, and establish a random path through all of the unsampled location in a way that each location to be simulated once only.

(a) At a location x_m' in the random path, the indicator variogram is used in the IK estimator to estimate the probability of toxic metals concentrations being lower than a given cutoff value z_k:

$$F\left[z_k; x_m' | (n + m - 1) \right] = \sum_{i=1}^{n+m-1} \lambda_i I(x_i; z_k) = Prob_{IK}\left[z(x_m') \le z_k \right] \quad (9)$$

where λ_i are the weights; n is the number of observed data and $m-1$ is the number of previous simulated values. That is, the indicator codes $I(x; z_k)$ of the $m-1$ previous simulated values of the locations in the random path should be added in the IK estimation of the next location x_m'.

(b) Build the prior continuous conditional cumulative distribution function (ccdf) for the location x_m' with the several probability values respectively corresponding to the given cutoff values z_k.

(c) Randomly draw a simulated value $z(x_m')$ from the prior ccdf for the location x_m'. Add the indicator code of $z(x_m')$ in the Eq. (9) for modeling the prior ccdf of the next location x_{m+1}'.

(4) Repeat the previous steps (a)–(c) to proceed along the random path to obtain a joint realization for unsampled locations.

These sequential steps build up only one realization of the toxic metals spatial distribution. Multiple realizations can be yielded with various random paths. Each realization gives a random path and obtains an outcome of the spatial distribution of toxic metals concentrations, thus the uncertainty of mapping can be obtained through many realizations.

2.6. Uncertainty analysis of simulated results

The main objective of this study is to detect areas that are potentially hazardous to human health. And the accepted safe level (1) was used to determine the potential hazardous areas of toxic metal. The probability that unknown toxic metal $HI(x')$ at x' is greater than the critical limit (1), denoted by Prob $[HI(x') > 1]$, can be calculated based on the following equation (Goovaerts, 2001; Juang et al., 2004):

$$Prob[HI(x') > 1] = \frac{n(x')}{N_{SIS}} \quad (10)$$

The $n(x')$ is the number of realizations where the simulated $HI(x')$ value exceeds the accepted safe level (1). And the N_{sis} is the number of realizations used in this study.

3. Results and discussion

3.1. Description statistics of soil toxic metals and soil properties

A summary of the soil properties, with basic statistical data for the samples is given in Table S2. The histograms and the summary data (such as mean, median, maximum, minimum, upper quartile, lower quartile, standard deviation, coefficients of variation and skewness) of two toxic metals concentrations for 52 samples are shown in Fig. 3. Both the soil background values for Hunan province (Pan and Yang, 1988) and the guideline values of the Chinese Environmental Quality Standard for Soils (MEPPRC, 1995) were used as the reference values. According to the current Chinese Environmental Quality Standard for Soils (MEPPRC, 1995), the second class values generally are developed for protecting agricultural production and corresponding human health (MEPPRC, 1995) which are often used for identifying pollution state of soil toxic metals. The mean concentration of Cr was 85.7 mg/kg, which was higher than its soil background values for Hunan (68 mg/kg), meaning Cr was enriched in the topsoil. However, the mean concentration of Pb was 26. 7 mg/kg, which was near by its background values for Human (30 mg/kg), indicating that there was no

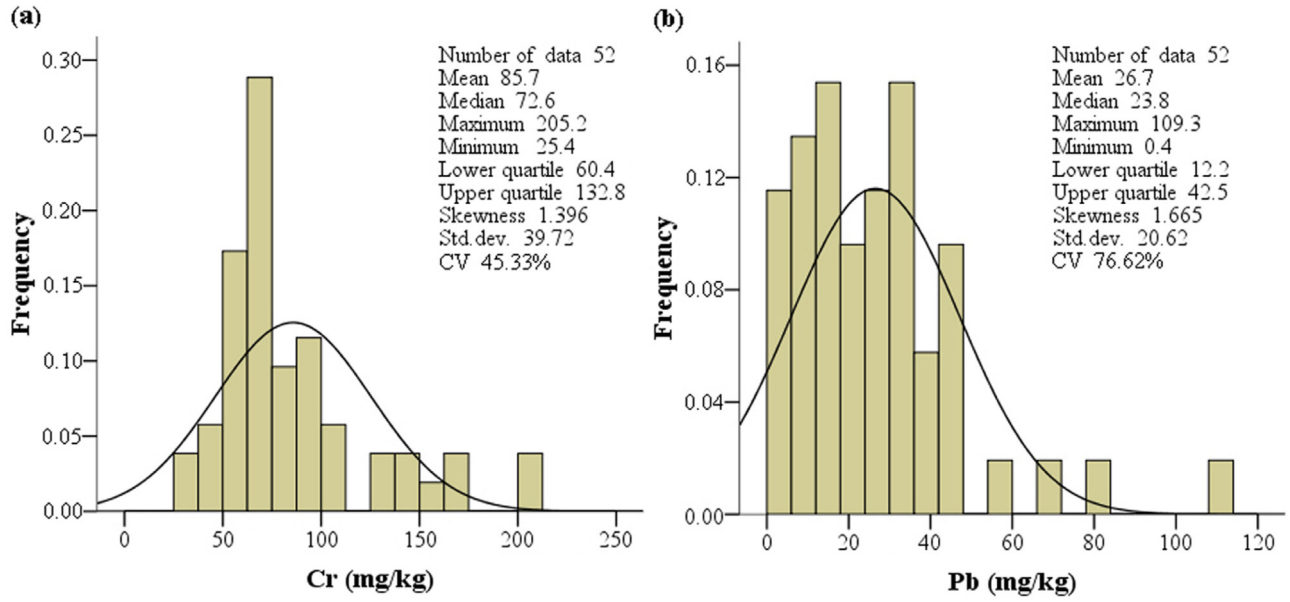

Fig. 3. Frequency histograms and summary data of Cr and Pb for 52 soil samples.

Table 1
SIS simulation parameters of variogram models for toxic metals with four thresholds.

	Threshold	Percentile (%)	Model	C_0	$C+C_0$	$C_0/(C_0+C)$	Range (km)	RSS	r^2
Cr	57.7	20	Spherical	0.0301	0.1602	0.187	14.5	0.0098	0.804
	69.2	40	Spherical	0.0569	0.3378	0.168	38.22	0.0201	0.781
	78.9	60	Exponential	0.0310	0.2462	0.125	11.94	0.0362	0.468
	108	80	Spherical	0.0165	0.1670	0.098	9.75	0.0188	0.446
Pb	10.5	20	Spherical	0.0301	0.1552	0.193	5.06	0.0249	0.434
	18	40	Spherical	0.0312	0.2410	0.129	8.22	0.0196	0.770
	29.4	60	Spherical	0.0370	0.2590	0.142	4.19	0.0108	0.778
	39.2	80	Spherical	0.0555	0.1540	0.360	4.28	0.0151	0.955

apparent Pb enrichment in the studied area. The coefficients of variation (CV) of Cr and Pb were 45.33% and 76.62%, which indicated the moderate to great spatial variation of Cr and Pb. At the same time, it also meant that these Cr and Pb in topsoil were affected by the local anthropogenic activities (e.g. chemical production, transportation and manufacturing). Though both the peak concentrations of Cr and Pb did not exceed the Class II of the Environmental Quality Standard for soils in China (250 mg/kg for Cr and Pb) (MEPPRC, 1995), several locations presented Cr and Pb concentrations much higher than the soil background values for Hunan province, meaning that the soil in some areas may exhibit a pollution trend. And in our previous study (Li et al., 2015b), we found that Class II of the Environmental Quality Standard for soils in China could not be suitable for protecting urban population safety. Therefore, it is inappropriate to deem the Cr and Pb in soil of XDD 'safe' for local people and the health risk assessment of Cr and Pb in soil of XDD is necessary.

3.2. Spatial distribution of soil toxic metals concentrations

According to procedure of SIS, four thresholds (20, 40, 60 and 80 percentile) were used to perform the indicator transformation of Cr and Pb. For no apparent anisotropy was found for Cr and Pb data, experimental variograms were estimated omni-directly. Isotropic variogram models based on the original Cr and Pb data were fitted using GS+7.0 and the corresponding variogram model parameters were listed in Table 1. The nugget-to-still ration $C_0/(C_0+C)$ is a criterion and usually used to define distinct classes of spatial dependence for the soil variables. If the ratio was lower than 25%, the variable was considered strongly spatially dependent; if the ratio was between 25% and 75%, the variable was considered moderately spatially dependent; and if the ratio was higher than 75%, the variable was considered weakly spatially dependent (Cambardella et al., 1994; Qu et al., 2013a). Generally, strong spatial dependence of soil properties may be due to intrinsic factors and weak spatial dependence may result from extrinsic factors (Cambardella et al., 1994; Qu et al., 2013a). The nugget-to-still rations $C_0/(C_0+C)$ of the variogram model for indicator transformed Cr data were 9.8–18.7%, exhibiting strong spatial auto dependency. Meanwhile, the nugget-to-still rations $C_0/(C_0+C)$ of the variogram model for indicator transformed Pb data were 12.9–36.0%, exhibiting moderate to strong spatial auto dependency which may be attributed to intrinsic factors such as other soil properties and extrinsic factors such as human activities.

Based on the parameters listed in Table 1, 1000 realizations of Cr and Pb exposure concentrations in soil were respectively simulated using the GSLIB90 SISIM routine (Deutsch and Journel, 1998) on a 200×200 m square grid. Each realization was equiprobable. Fig. 4 showed the average concentrations, also known as E-type estimates, of Cr and Pb obtained by averaging the 1000 realizations based on the original data. These maps reflected the global distribution trends of Cr and Pb in the topsoil of XDD. For Cr

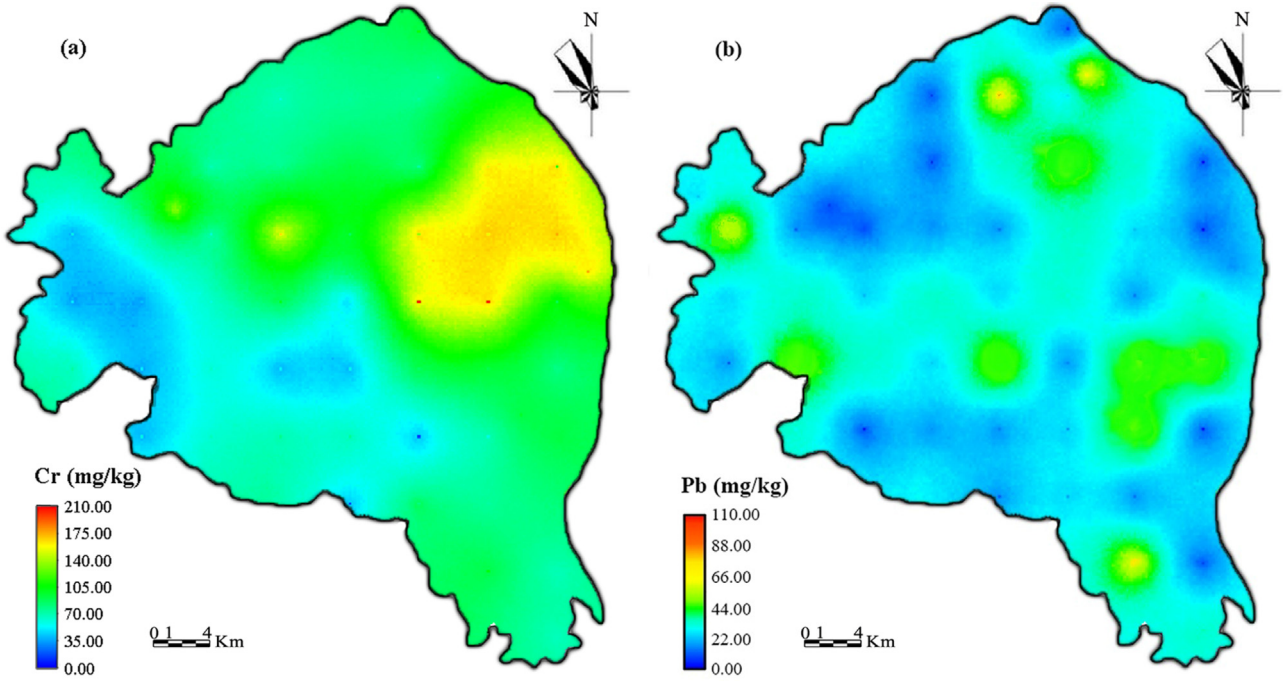

Fig. 4. Spatial distribution maps of (a) Cr and (b) Pb in the topsoil of XDD.

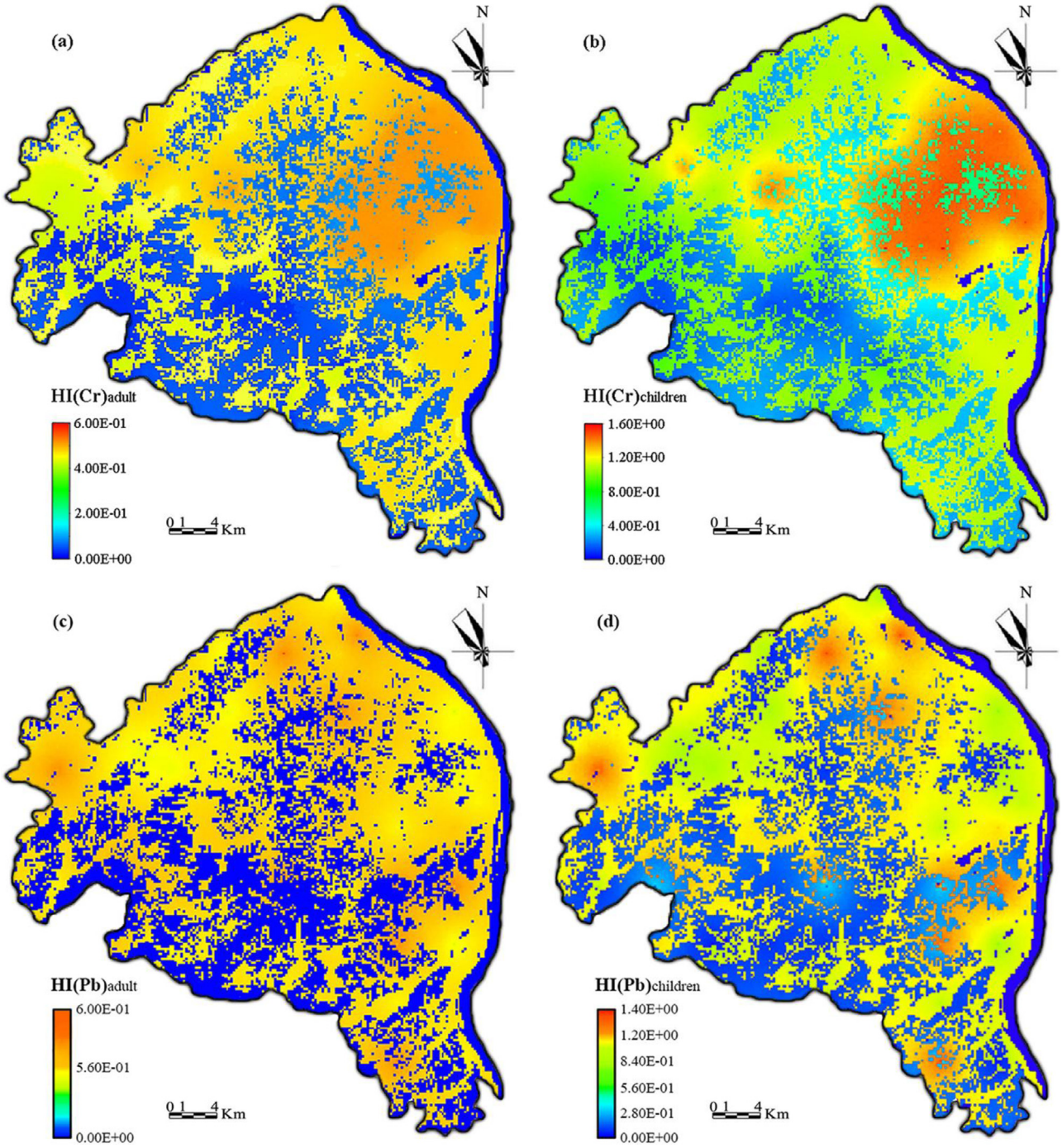

Fig. 5. Spatial distribution maps of *HI* of (a), (b) Cr and (c), (d) Pb in the topsoil of XDD.

(Fig. 4a), the higher values appeared in the east region and lower values mainly occurred in the southwest region of the XDD. Printery, alloy melting factories and coal mining activities often cause Cr contamination (Wang et al., 2010; Chen et al., 2011). The higher values appeared in the east region may be mainly due to industrial activities in the area. According to Fig. 4b, the higher values of Pb were spatially scattered in the areas around F1, F4, F6, F8, F13, F14, U5, U14, W2 and W11. According to previous studies (Wang et al., 2010; Chen et al., 2011), the high Pb content in some parts of XDD may caused by non-ferrous metal mining, mineral processing and smelting in these areas. Comparing Figs. 1 and 4, the estimates for study metals (Cr and Pb) and the land use in XDD showed similar spatial patterns, with large Cr and Pb concentrations mainly located in farm and residential land. This indicated that the soil Cr and Pb contents might be correlated with land use types in XDD to a certain extent. Therefore, land use types in the XDD should be taken into account in the process of human health risk assessment.

3.3. Spatial human health risk associated with different land uses

The current land uses in the study area were showed in Fig. 2, including farm land, forest land, residential land and water area. The forested areas were mainly located on the center, south and southwest of XDD. The water areas mainly comprised parts of Xiangjiang in the east, Weishui in the north and small ponds

scattered in the east of XDD. The farm land was mainly distributed on the flat alluvial land along the XiangJiang and Weishui rivers, while the residential land was scattered throughout the farm land. The map data were firstly divided into 200 × 200 m grids using the ArcGIS 9.3, and then the rasterized map was linked to the simulation results of soil Cr and Pb.

According to Fig. 1, a series simulation of non-carcinogenic health risks of children and adults exposure to Cr and Pb were conducted based on the simulated results of Cr and Pb concentrations in topsoil and the rasterized land use types in the XDD referred above. Each simulation was equiprobable and a set of realizations can reveal the possible spatial distribution patterns of *HI* for Cr and Pb in the topsoil of XDD. In order to acquire a preliminary knowledge of the *HI* distribution trend of Cr and Pb to children and adults, as well as the priority pollutants/regions of concern under different land uses, the maps of E-type estimates obtained by averaging the 1000 realizations were plotted and showed in Fig. 5. For both Cr and Pb, a similar spatial distribution trend was observed for the E-type estimate *HI* values to adults in comparison to children, which suggested a positive correlation between the non-carcinogenic risk for adults and children. According to Fig. 5a, the E-type estimate *HI* values of Cr to adults at all study area did not exceed the accepted safe level (1). However, the E-type estimate *HI* values of Cr for children in about 30% area from XDD exceeded the accepted safe level (1) (Fig. 5b), and the higher risk areas were mainly in the east, north and north-east part, where the land use types are residential and farm land, indicating a potential human health risk to children in these areas. Comparing Fig. 4a and Fig. 5b, there were partly differences between the estimate concentrations and the estimate risks of Cr. Cr concentrations estimated around F7, U2 and W4 were relatively higher, while the estimated *HI* values of Cr to children around these points were under the accepted level (1). The areas around F4 and U7 exhibited low concentrations of Cr, but its corresponding *HI* values to children were relatively higher. For Pb, the maximum E-type estimate *HI* value to adults did not exceed 1.0 (Fig. 5c). However, the areas around F1, F4, F8, F14, U5, U10 and U14 were with a high non-carcinogenic risk of Pb to children. Compared to Fig. 4b, Pb concentrations estimated around F13, W2 and W11 were relatively higher, but the estimated *HI* values of Pb to children around these points were under the accepted level (1). And the areas around F7, F20 and U11 exhibited low concentrations of Pb, but its corresponding *HI* values for children were relatively higher. This difference indicated that the land use type had a significant effect on the non-carcinogenic health risk of Cr and Pb. The modeling in this study provided a more reasonable assessment of human health by integrating spatial analysis of contaminant concentrations and land use. The results were also in some difference from the analysis with reference of the Chinese Environmental Quality Standard for Soils (MEPPRC, 1995), indicating that current Environmental Quality Standard for Soils posed in 1995 could not be well fit for requirements of the present and need to be further revised. Cr can cause respiratory irritation, cancer, liver damage and pulmonary congestion (Broadway et al., 2010; Zhang et al., 2015). And excessive exposure to Pb may cause plumbism, anemia, nephropathy, gastrointestinal colic and central nervous system symptom (Zukowska and Biziuk, 2008). Children are more susceptible to lead poisoning than adults because of increased exposure through frequent hand–to–mouth activities, increased lead absorption by the gut compared to adults and increased vulnerability of their central nervous systems (Herbert, 2004; Ko et al., 2007; Stewart et al., 2014). Thus, Cr and Pb in the topsoil from XDD should be regarded as the priority pollutants of concern. And identification of detailed priority areas for Cr and Pb is necessary for making targeted risk management strategy.

3.4. Uncertainty evaluation and a hierarchical risk management policy

Fig. 6 showed the distribution, after 1000 simulations, of the probability of *HI* in excess of the accepted level (1) of Cr and Pb for children associated with different land uses. The probability map can be used to measure the reliability of delineating the hazardous zone based on a selected critical probability of each single location. A high value represents a high probability of hazardous zone, while the reverse means that the risk of the zone will be uncertain

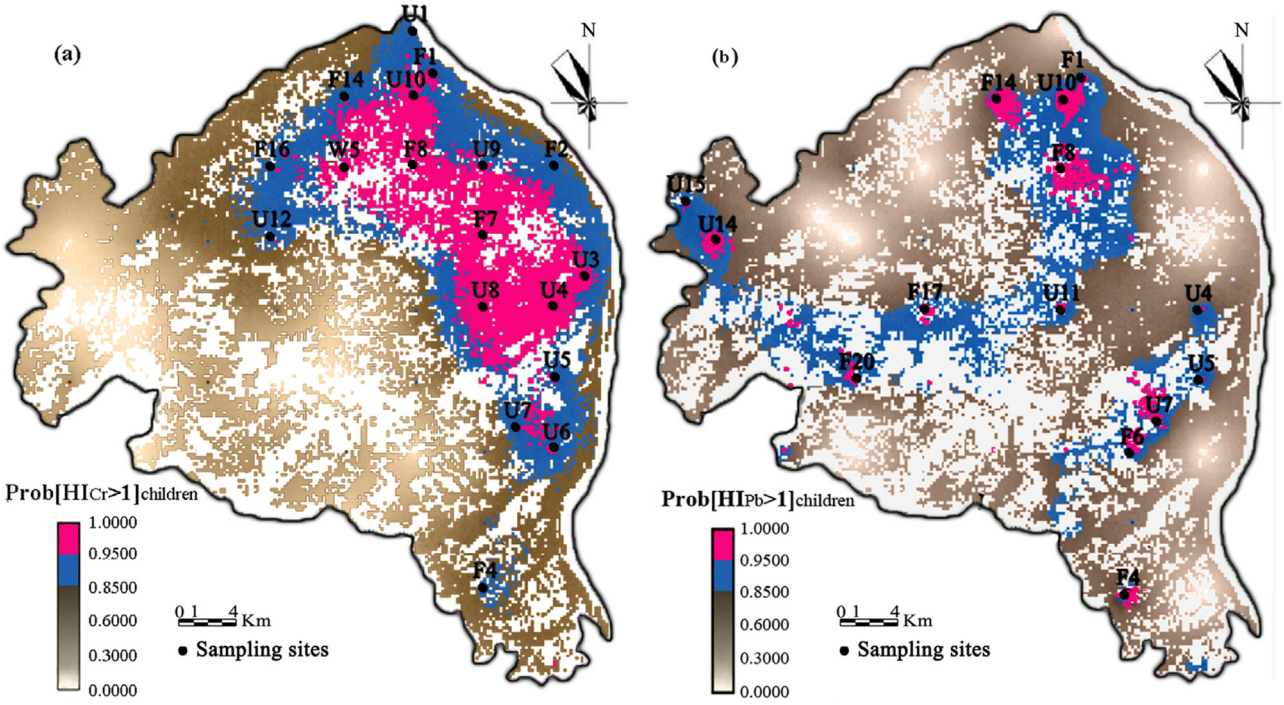

Fig. 6. Probability of risk of (a) Cr and (b) Pb in excess of the accepted level.

and more information is needed. According to Fig. 6, the areas with higher probability of *HI* for Cr were located in the east of the study area, where the land use types are residential and farm land. And for Pb, the areas with higher probability of *HI* were near sampling sites F1, F4, F8, F14, U5, U10 and U14. To provide more efficient information for policy-maker, two kinds of areas were delineated out based on the probability map given the suggested critical probabilities of 0.85 and 0.95. For validation, the areas with the probability of risk higher than 0.95 were highlighted in red, and with the probability of risk between 0.85 and 0.95 were highlighted in blue. The acreage of the areas with probability of risk higher than 0.95 for Cr and Pb were 148.32 km^2 (12% of XDD) and 37.08 km^2 (3% of XDD), respectively. And the acreage of the areas with probability of risk between 0.85 and 0.95 for Cr and Pb were 185.4 km^2 (15% of XDD) and 173.04 km^2 (14% of XDD), respectively. Comparing Figs. 5 and 6, it was found that the areas with non-carcinogenic risk of Cr and Pb to children in excess of the accepted level (1) approximated to the risk regions with probability above 0.85.

Based on Figs. 5 and 6, a hierarchical risk management policy was suggested to provide reference for flexible and cost-efficient risk management policy-making. According to the E-type *HI* values of Cr and Pb, the XDD was first divided into A, B and C regions with *HI* (A) > *HI* (B) > *HI* (C). E-type *HI* values of Cr and Pb in region A exceeded safe level (1). E-type *HI* values of Cr and Pb in region B were between 0.5 and 1. And in region C the E-type *HI* values of Cr and Pb did not exceed 0.5. With the limited budget consideration, a further layering based on the probability of risk in region A was suggested. The areas with high probability (> 0.95) in region A were suggested to be the first priority areas for both Cr and Pb. And preferentially environmental management and remediation were required at the same time with target control of the probable risk sources and worth for preferred budget support for the higher probability of exposure to receptors. While the areas with probability between 0.85 and 0.95 in region A were suggested to be the secondary priority areas for Cr and Pb. Because of a relatively large uncertainty of risk in the secondary priority areas, comprehensive risk management for the secondary priority areas was suggested as follow: (i) to make preliminary risk management in these areas; (ii) to conduct a further sampling, monitoring, and analysis to get more information of the non-carcinogenic risk of Cr and Pb, and to make focused management according to the results. Finally, for other areas for Cr and Pb, a regular sampling, monitoring and analysis were recommended, especially in the relative hotpots and the area with farm or residential land uses for mastering the change of toxic metal pollution state throughout XDD in time.

The evaluation of uncertainty is an important step accompanying the human health risk assessment. Some sources of uncertainty are well emphasized in the study of Li et al. (2012), such as the reference toxicity values and the exposure parameters associated with health risk assessment. In our current study, we temporarily assumed parameters associated with health risk assessment are certain. Therefore, it is recommended that a clinical toxicological research should be carried out in XDD, and a further investigation on the exposure parameters of children and adults living in different communities of XDD to topsoil are recommended to be performed. And with some limitations of the SIS (Gotway et al., 1994; Emery, 2004), a further work can be done in the evaluation of soil toxic metals concentrations. Furthermore, other factors, including contamination variation, combined pollution and the local population size are also not considered in this study. Though there are some uncertainties, the present study would pose a useful tool to assess the human health risk associated with different land uses using SIS and could help to supply detailed and hierarchical information to the public or government about detailed priority pollutants/regions of concern.

4. Conclusions

The method modified in this study took the spatial distribution and local uncertainty of Cr and Pb concentrations into account and incorporated different exposure models and current land use types in the study area to assess spatial human health risk. The concentrations of Cr and Pb in topsoil of XDD were investigated, and the values of Cr and Pb at several locations were higher than their local soil background values, indicating an anthropogenic input. Spatial patterns of Cr and Pb concentrations in soil are simulated using SIS. The higher values of Cr appeared in the east region and lower values were mainly located in the southwest region of the XDD. And the higher values of Pb were spatially scattered in the areas around F1, F6, F8, F13, F14, U5, U14, W2 and W11. The estimates for study metals (Cr and Pb) and the land use in XDD showed similar spatial patterns, meaning the soil Cr and Pb contents might be correlated with land use types in XDD to a certain extent. Based on the simulated concentrations of Cr and Pb and the land use types extracted by remote-sensing software, the spatial distribution of E-type *HI* values of Cr and Pb was evaluated and their probability of risk in excess of the accepted level (1) were mapped. The results showed that E-type *HI* values of Cr and Pb to adults overall XDD did not exceed the accepted safe level (1). However, around some areas, Cr and Pb exhibited *HI* larger than the safe level (1) to children. Therefore, Cr and Pb should be regarded as priority pollutants of concern.

To identify the detailed priority regions of concern, a hierarchical risk management policy, which incorporated the E-type risk map and its probability of risk map, was proposed. And the results suggested the areas with high probability (> 0.95) in region A should be regard as the first priority areas of concern for Cr and Pb, where preferential environmental management and targeted pollution source control were required. While the areas with probability between 0.85 and 0.95 in region A were suggested to be the secondary priority areas for Cr and Pb. With the limited budget consideration, preliminary risk management was required and a further sampling, monitoring and analysis were also recommended to make a further focused management in the secondary priority areas.

Acknowledgments

This study was financially supported by the National Natural Science Foundation of China (51178172, 51039001, 51308076, 51378190, 51521006 and 51578222), the Project of Chinese Ministry of Education (113049A) and the Research Fund for the Program for Changjiang Scholars and Innovative Research Team in University (IRT-13R17).

Appendix A. Supplementary material

Supplementary data associated with this article can be found in the online version at http://dx.doi.org/10.1016/j.ecoenv.2016.03.029.

References

Boularbah, A., Schwartz, C., Bitton, G., Morel, J.L., 2006. Heavy metal contamination from mining sites in South Morocco: 1. Use of a biotest to assess metal toxicity of tailings and soils. Chemosphere 63, 802–810.

Broadway, A., Cave, M.R., Wragg, J., Fordyce, F.M., Bewley, R.J., Graham, M.C., Ngwenya, B.T., Farmer, J.G., 2010. Determination of the bioaccessibility of chromium in Glasgow soil and the implications for human health risk assessment. Sci. Total Environ. 409, 267–277.

Cai, L.M., Xu, Z.C., Qi, J.Y., Feng, Z.Z., Xiang, T.S., 2015. Assessment of exposure to

heavy metals and health risks among residents near Tonglushan mine in Hubei, China. Chemosphere 127, 127–135.
Cambardella, C.A., Moorman, T.B., Novak, J.M., Parkin, T.B., Karlen, D.L., Turco, R.F., Konopka, A.E., 1994. Field-scale variability of soil properties in Central Iowa soils. Soil Sci. Soc. Am. J 58, 1501–1511.
Chen, J., Wang, Z., Wu, X., Zhu, J., Zhou, W., 2011. Source and hazard identification of heavy metals in soils of Changsha based on TIN model and direct exposure method. Trans. Nonferr. Met. Soc. 21, 642–651.
Cheng, Y., Nathanail, P.C., 2009. Generic Assessment Criteria for human health risk assessment of potentially contaminated land in China. Sci. Total Environ. 408, 324–339.
Deutsch, C., Journel, A., 1998. GSLIB: Geostatistical Software Library And User's Guide, second ed. Oxford University Press Inc., New York.
Emery, X., 2004. Properties and limitations of sequential indicator simulation. Stoch. Environ. Res. Risk Assess. 18, 414–424.
Gay, J.R., Korre, A., 2006. A spatially-evaluated methodology for assessing risk to a population from contaminated land. Environ. Pollut. 142, 227–234.
Gay, J.R., Korre, A., 2009. Accounting for pH heterogeneity and variability in modelling human health risks from cadmium in contaminated land. Sci. Total Environ. 407, 4231–4237.
Gotway, C., Rutherford, A., B., M., 1994. Stochastic simultation for imaging spatial uncertainty: comparison and evaluation of available algorithms. In: Armstrong, M., Dowd, P., A. (Eds.), Geostatistical Simulations. Fontainebleau, France, pp. 1–21.
Goovaerts, P., 1996. Stochastic simulation of categorical variables using a classification algorithm and simulated annealing. Math. Geol. 28, 909–921.
Goovaerts, P., 1997. Geostatistics for Natural Resources Evaluation. Oxford University Press, New York.
Goovaerts, P., 2001. Geostatistical modelling of uncertainty in soil science. Geoderma 103, 3–26.
Guney, M., Zagury, G.J., Dogan, N., Onay, T.T., 2010. Exposure assessment and risk characterization from trace elements following soil ingestion by children exposed to playgrounds, parks and picnic areas. J. Hazard. Mater. 182, 656–664.
Guo, G., Wu, F., Xie, F., Zhang, R., 2012. Spatial distribution and pollution assessment of heavy metals in urban soils from southwest China. J. Environ. Sci. 24, 410–418.
Guo, X., Komnitsas, K., Li, D., 2010. Correlation between herbaceous species and environmental variables at the abandoned Haizhou coal mining site. Environ. Forensics 11, 146–153.
Herbert, N., 2004. Lead Poisoning. Annu. Rev. Med. 55, 209–222.
Huang, J., Li, F., Zeng, G., Liu, W., Huang, X., 2016. Integrating hierarchical bioavailability and population distribution into potential eco-risk assessment of heavy metals in road dust: a case study in xiandao district, Changsha city, China. Sci. Total Environ. 541, 969–976.
Islam, S., Ahmed, K., Al-Mamun, H., 2015. Distribution of trace elements in different soils and risk assessment: a case study for the urbanized area in Bangladesh. J. Geochem. Explor. 158, 212–222.
Ji, K., Kim, J., Lee, M., Park, S., Kwon, H.J., Cheong, H.K., Jang, J.Y., Kim, D.S., Yu, S., Kim, Y.W., Lee, K.Y., Yang, S.O., Jhung, I.J., Yang, W.H., Paek, D.H., Hong, Y.C., Choi, K., 2013. Assessment of exposure to heavy metals and health risks among residents near abandoned metal mines in Goseong, Korea. Environ. Pollut. 178, 322–328.
Juang, K.W., Chen, Y.S., Lee, D.Y., 2004. Using sequential indicator simulation to assess the uncertainty of delineating heavy-metal contaminated soils. Environ. Pollut. 127, 229–238.
Ko, S., Schaefer, P.D., Vicario, C.M., Binns, H.J., 2007. Relationships of video assessments of touching and mouthing behaviors during outdoor play in urban residential yards to parental perceptions of child behaviors and blood lead levels. J. Expo. Sci. Epidemiol. 17, 47–57.
Komnitsas, K., Modis, K., 2009. Geostatistical risk assessment at waste disposal sites in the presence of hot spots. J. Hazard. Mater. 164, 1185–1190.
Korre, A., Durucan, S., Koutroumani, A., 2002. Quantitative-spatial assessment of the risks associated with high Pb loads in soils around Lavrio, Greece. Appl. Geochem. 17, 1029–1045.
Lei, M., Tie, B., Williams, P.N., Zheng, Y., Huang, Y., 2010. Arsenic, cadmium, and lead pollution and uptake by rice (Oryza sativa L.) grown in greenhouse. J. Soil. Sedim. 11, 115–123.
Li, F., Huang, J., Zeng, G., Huang, X., Li, X., 2014. Integrated source apportionment, screening risk assessment, and risk mapping of heavy metals in surface sediments: a case study of the Dongting Lake, Middle China. Hum. Ecol. Risk Assess. 20, 1213–1230.
Li, F., Huang, J., Zeng, G., Huang, X., Liu, W., Wu, H., Yuan, Y., He, X., Lai, M., 2015a. Spatial distribution and health risk assessment of toxic metals associated with receptor population density in street dust: a case study of Xiandao District, Changsha, Middle China. Environ. Sci. Pollut. Res. 22, 6732–6742.
Li, F., Huang, J., Zeng, G., Liu, W., Huang, X., Huang, B., Gu, Y., Shi, L., He, X., He, Y., 2015b. Toxic metals in topsoil under different land uses from Xiandao District, middle China: distribution, relationship with soil characteristics, and health risk assessment. Environ. Sci. Pollut. Res. 22, 12261–12275.
Li, F., Huang, J., Zeng, G., Yuan, X., Li, X., 2013. Spatial risk assessment and sources identification of heavy metals in surface sediments from the Dongting Lake, Middle China. J. Geochem. Explor. 132, 75–83.
Li, F., Huang, J., Zeng, G., Yuan, X., Liang, J., Wang, X., 2012. Multimedia health impact assessment: a study of the scenario-uncertainty. J. Cent. South Univ. 19, 2901–2909.
Li, M.D., Tang, H.T., Tang, R., Zhang, Y.Y., 2005. The investigation and evaluation of heavy metal state from soil and vegetable in the suburb of Changsha Region. Hunan Agric. Sci., 34–36.
Li, P., Lin, C., Cheng, H., Duan, X., Lei, K., 2015c. Contamination and health risks of soil heavy metals around a lead/zinc smelter in southwestern China. Ecotoxicol. Environ. Saf. 113, 391–399.
Lim, H., Lee, J., Chon, H., Sager, M., 2009. Heavy metal contamination and health risk assessment in the vicinity of the abandoned Songcheon Au–Ag mine in Korea. J. Geochem. Explor. 96, 223–230.
Liu, H., Probst, A., Liao, B., 2005. Metal contamination of soils and crops affected by the Chenzhou lead/zinc mine spill (Hunan, China). Sci. Total Environ. 339, 153–166.
Liu, J.H., Chen, Y.C., 2004. Primary investigation on contamination pattern of vegetables by heavy metals in chinese cities. Stud. Trace Elem. Health 21, 42–44.
MAPRC, 2006. Soil Testing (NY/T 1121.1～12-2006). Ministry of Agriculture of the People's Republic of China, Beijing (in Chinese).
MEPPRC, 1995. Environmental Quality Standard for Soils, GB 15618-1995. Ministry of Environmental Protection of the People's Republic of China, Beijing (in Chinese).
MEPPRC, 2014. Technical Guidelines for Risk Assessment of Contaminated Sites, HJ 25.3-2014. Ministry of Environmental Protection of the People's Republic of China, Beijing (in Chinese).
Modis, K., Papantonopoulos, G., Komnitsas, K., Papaodysseus, K., 2008. Mapping optimization based on sampling size in earth related and environmental phenomena. Stoch. Env. Res. Risk Assess. 22, 83–93.
Pan, Y.M., Yang, G.Z., 1988. Hunan Soil Background Values and Research Mehods. Chinese Environmental Science Press, Beijing (in Chinese).
Qu, M., Li, W., Zhang, C., 2013a. Assessing the risk costs in delineating soil nickel contamination using sequential Gaussian simulation and transfer functions. Ecol. Inform. 13, 99–105.
Qu, M., Li, W., Zhang, C., 2013b. Assessing the spatial uncertainty in soil nitrogen mapping through stochastic simulations with categorical land use information. Ecol. Inform. 16, 1–9.
Saleem, M., Iqbal, J., Shah, M.H., 2014. Non-carcinogenic and carcinogenic health risk assessment of selected metals in soil around a natural water reservoir, Pakistan. Ecotoxicol. Environ. Saf. 108, 42–51.
Simasuwannarong, B., Satapanajaru, T., 2012. Spatial Distribution and Risk Assessment of As, Cd, Cu, Pb, and Zn in Topsoil at Rayong Province, Thailand. Water Air Soil Pollut. 223, 1931–1943.
Stewart, L.R., Farver, J.R., Gorsevski, P.V., Miner, J.G., 2014. Spatial prediction of blood lead levels in children in Toledo, OH using fuzzy sets and the site-specific IEUBK model. Appl. Geochem. 45, 120–129.
United Nations, Department of Economic and Social Affairs, Population Division, 2014. World Urbanization Prospects: The 2014 Revision, Highlights (ST/ESA/SER.A/352).
US Department of Energy, 2004. RAIS: risk assessment information system. US Department of Energy, Washington DC.
US EPA, 1989. Risk Assessment Guidance for Superfund Human Health Evaluation Manual (part A) vol. I (EPA/540/1-89/002).
US EPA, 1996. Soil Screening Guidance: Technical Background Document (EPA/540/R-95/128). US Environmental Protection Agency, Washington DC.
US EPA, 2002. Supplemental guidance for developing soil screening levels for superfund sites (OSWER 9355.4-24). US Environmental Protection Agency, Washington DC.
Wang, Z., Chai, L., Yang, Z., 2010. Identifying sources and assessing potential risk of heavy metals in soils from direct exposure to children in a mine-impacted city, Changsh, China. J. Environ. Qual. 39, 1616–1623.
Wang, L., Lu, X., Ren, C., Li, X., Chen, C., 2014. Contamination assessment and health risk of heavy metals in dust from Changqing industrial park of Baoji, NW China. Environ. Earth Sci. 71, 2095–2104.
Xi, D., Sun, Y., Liu, X., 2004. Environmental Monitoring, 3rd edition. Higher Education Press, Beijing (in Chinese).
Xiao, Q., Zong, Y., Lu, S., 2015. Assessment of heavy metal pollution and human health risk in urban soils of steel industrial city (Anshan), Liaoning, Northeast China. Ecotox. Environ. Saf. 120, 377–385.
Xu, J., Sharma, R., Fang, J., Xu, Y., 2008. Critical linkages between land-use transition and human health in the Himalayan region. Environ. Int. 34, 239–247.
Yuan, G.L., Sun, T.H., Han, P., Li, J., Lang, X.X., 2014. Source identification and ecological risk assessment of heavy metals in topsoil using environmental geochemical mapping: typical urban renewal area in Beijing, China. J. Geochem. Explor. 136, 40–47.
Zeng, G., Liang, J., Guo, S., Shi, L., Xiang, L., Li, X., Du, C., 2009. Spatial analysis of human health risk associated with ingesting manganese in Huangxing Town, Middle China. Chemosphere 77, 368–375.
Zhang, L., Mo, Z., Qin, J., Li, Q., Wei, Y., Ma, S., Xiong, Y., Liang, G., Qing, L., Chen, Z., Yang, X., Zhang, Z., Zou, Y., 2015. Change of water sources reduces health risks from heavy metals via ingestion of water, soil, and rice in a riverine area, South China. Sci. Total Environ. 530–531, 163–170.
Zhao, H., Xia, B., Fan, C., Zhao, P., Shen, S., 2012. Human health risk from soil heavy metal contamination under different land uses near Dabaoshan Mine, Southern China. Sci. Total Environ. 417-418, 45–54.
Zhao, L., Xu, Y., Hou, H., Shangguan, Y., Li, F., 2014. Source identification and health risk assessment of metals in urban soils around the Tanggu chemical industrial

district, Tianjin, China. Sci. Total Environ. 468–469, 654–662.
Zhao, Y., Shi, X., Yu, D., Wang, H., Sun, W., 2005. Uncertainty assessment of spatial patterns of soil organic carbon density using sequential indicator simulation, a case study of Hebei province, China. Chemosphere 59, 1527–1535.
Zhao, Y., Xu, X., Sun, W., Huang, B., Darilek, J.L., Shi, X., 2008. Uncertainty assessment of mapping mercury contaminated soils of a rapidly industrializing city in the Yangtze River Delta of China using sequential indicator co-simulation. Environ. Monit. Assess. 138, 343–355.
Zukowska, J., Biziuk, M., 2008. Methodological evaluation of method for dietary heavy metal intake. J. Food Sci. 73, R21–R29.